Organic Electronics 32 (2016) 115–119

Contents lists available at ScienceDirect

Organic Electronics

journal homepage: www.elsevier.com/locate/orgel

Indium-tin-oxide, free, flexible, nonvolatile memory devices based on graphene quantum dots sandwiched between polymethylsilsesquioxane layers

Poh Choon Ooi [a, b, 1], Jian Lin [b, 1], Tae Whan Kim [a, *], Fushan Li [b, **]

[a] Department of Electronics and Computer Engineering, Hanyang University, Seoul 133-791, South Korea
[b] Institute of Optoelectronic Display, Fuzhou University, Fuzhou 350002, PR China

ARTICLE INFO

Article history:
Received 29 December 2015
Received in revised form
3 February 2016
Accepted 14 February 2016
Available online xxx

Keywords:
Flexible
Nonvolatile memory device
Graphene quantum dot
Polymethylsilsesquioxane
Electrical characteristic
Conduction mechanism

ABSTRACT

Indium-tin-oxide (ITO) free, nonvolatile memory (NVM) devices based on graphene quantum dots (GQDs) sandwiched between polymethylsilsesquioxane (PMSSQ) layers were fabricated directly on polyethylene terephthalate (PET) substrates by using a solution process technique. Current-voltage (*I-V*) curves for the silver nanowire/PMSSQ/GQD/PMSSQ/poly(3,4-ethylenethiophene):poly(styrene sulfonate)/PET devices at 300 K showed a current bistability. The ON/OFF ratio of the current bistability for the NVM devices was as large as 1×10^4, and the cycling endurance time of the ON/OFF switching for the NVM devices was above 1×10^4 s. The Schottky emission, Poole-Frenkel emission, trapped-charge limited-current, and space-charge-limited current were dominantly attributed to the conduction mechanisms for the fabricated NVM devices based on the obtained *I-V* characteristics, and energy band diagrams illustrating the "writing" and the "erasing" processes of the devices.

1. Introduction

Optically transparent and mechanically flexible electronic devices, due to their having potentially promising impacts in the areas of transparency and flexibility, have recently emerged as excellent candidates for potential applications in next-generation electronic and optoelectronic systems, such as displays, energy storage devices, ultraviolet detectors, photovoltaic cells, and disposable electronics [1–5]. Solution-processing deposition methods have been particularly attractive because of interest in realizing transparent and flexible electronic devices without the need of complicated fabrication processes that require expensive vacuum equipment, high-temperature fabrication steps and high-manufacturing cost. Electronic and optoelectronic devices have been typically fabricated by using spin-coating, spray-coating, inkjet printing, and roll-to-roll printing methods [6–8]. Spin-coating and spray-coating deposition methods have been used to fabricate two-terminal, nonvolatile memory (NVM) devices, including top and bottom contact electrodes, in order to realize fully solution-processed NVM devices in this study.

The top contact electrodes can be formed by using spray-coating techniques, instead of an expensive and time-consuming metal vacuum evaporation process to deposit silver nanowires (Ag NWs) [6]. The commonly-used bottom conductive indium-tin-oxide (ITO) layer has been replaced by a conductive polymer poly(3,4-ethylenethiophene):poly(styrene sulfonate) (PEDOT:PSS) layer because the price of the ITO electrode has been dramatically increasing due to its limited availability and because ITO is mechanically brittle and has poor adhesion to organic materials [9–11]. Furthermore, the ITO film has some inherent problems, for instance, the release of oxygen and indium into the organic layer, poor transparency in the blue spectral region, and requirement for a high-temperature process to achieve complete crystallization [9,10].

Graphene quantum dots (GQDs) are used as a charge-trapping medium owing to their excellent properties, such as superior chemical inertness, low toxicity, and higher work function [12,13]. In addition, the quantum confinement effect and the boundary effect of GQDs make them a favorable charge-trapping medium

* Corresponding author.
** Corresponding author.
E-mail addresses: twkim@hanyang.ac.kr (T.W. Kim), fushanli@hotmail.com (F. Li).
[1] These authors contributed equally to this work.

http://dx.doi.org/10.1016/j.orgel.2016.02.020
1566-1199/

[14]. Organic/inorganic polymethylsilsesquioxane (PMSSQ) hybrid materials have been preferred as a dielectric layer for NVM devices based on GQDs because hybrid materials represent a novel class of materials in which the desirable physical properties of both organic and inorganic materials may be combined [15,16]. PMSSQ films were chosen in this work as dielectric layers due to their excellent thermal, mechanical, electronic, and optical properties, with potential applications to electronic devices. PMSSQ is solution processable and has a viscosity that can be adjusted to match the requirements for various thin-film solution deposition techniques [17]. Even though some investigations of the electrical characteristics of flexible NVM devices fabricated with GQDs by using a solution process method have been conducted [18], studies on the device performances of ITO-free NVM devices based on GQDs have not yet been performed.

This paper reports data for ITO-free NVM devices based on GQDs sandwiched between PMSSQ layers fabricated by using a solution process. Transmission electron microscopy (TEM) measurements were conducted to investigate the microstructural properties of the GQDs. Current-voltage (I–V) measurements were performed to investigate the current bistability for the devices. The retention characteristics of the ON and the OFF current states for the devices were measured to investigate the stability of each current state. The conduction mechanisms of the Ag NW/PMSSQ/GQD/PMSSQ/PEDOT:PSS/polyethylene terephthalate (PET) devices were described by using an energy-band diagram and the I–V results.

2. Experimental details

GQDs in deionized water (0.8 mg/ml) used in this study were supplied by the Ocean University of China and TEM image in Fig. 1 shows that the sizes of the GQDs ranged from 8 to 15 nm. The detailed preparation process for the PMSSQ solution is described elsewhere [19]. Two metal-insulator-metal (MIM), NVM devices with structures of (a) Ag NW/PMSSQ/PEDOT:PSS/PET and (b) Ag NW/PMSSQ/GQD/PMSSQ/PEDOT:PSS/PET, denoted as MIM-A and MIM-B, respectively, were fabricated, and their schematics are shown in Fig. 2(a) and (b). The fabrication of MIM-B began with a 5-W oxygen plasma treatment for 5 s being performed on a PET substrate with an area of 1.5 cm × 1.5 cm to ensure uniform dispersion of the conductive polymer. A PEDOT:PSS aqueous solution (Clevios PH1000) was spin-coated at 3000 rpm for 60 s, followed by the use of a drop-method film treatment to drop 120 μl of methanol on the film at 130 °C before annealing. Then, the film was annealed for 20 min to remove the hydrophilic insulator PSS from the film, thus producing a PEDOT:PSS film with enhanced conductivity, as reported in the literature [10]. Sequentially, the first PMSSQ layer was deposited on the treated PEDOT:PSS layer by spin-coating at 2000 rpm for 100 s, after which the sample was thermally cured at 160 °C for 1 h. Before spin-coating the GQDs at 2000 rpm for 60 s, a 5-W oxygen plasma treatment was performed for 5 s in order to reduce the hydrophobicity of the PMSSQ layer. Then, a PMSSQ layer was deposited by spin-coating at 6000 rpm for 100 s and subsequently cured at 160 °C for 1 h. Here, the reference sample without GQDs, MIM-A, was fabricated with two layers of PMSSQ deposited at the same rotational speed for the same time as were used for the experimental device, MIM-B. Finally, Ag NWs in isopropyl alcohol (IPA) (0.5 mg/ml) were spray-coated with the aid of shadow mask to form 0.5-mm-diameter circular top electrodes at 0.1 MPa on a hot plate at 100 °C.

I–V measurements on the memory devices were performed at room temperature to investigate the electrical properties of the fabricated two-terminal, MIM, NVM devices by using a semiconductor characterization system (Keithley 4200-SCS), and bias voltages were applied to the top metal electrode with respect to the ITO electrode for all measurements at a 0.1 A compliance current. A Shimadzu UV–VIS-NIR spectrophotometer (UV-3600) was used to measure the transparency of the NVM devices.

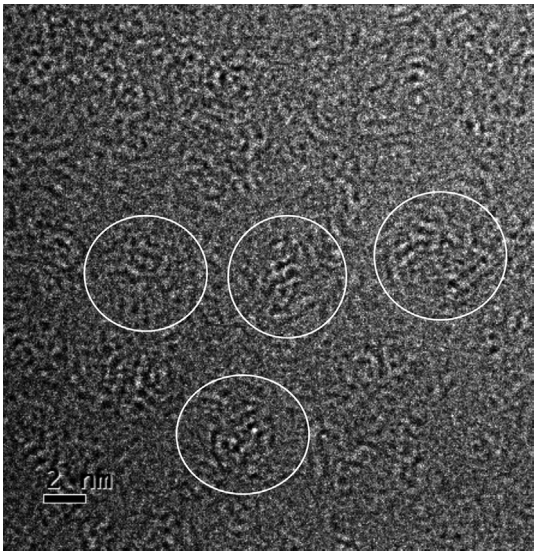

Fig. 1. Transmission electron microscopy image of graphene quantum dots (GQDs). The circles in Fig. 1 represent GQDs.

3. Results and discussion

Fig. 3 shows the transparency of the fabricated MIM, NVM devices in the visible spectral range from 400 to 800 nm. The absolute transmittance of the blank PET (blue solid line) is seen to vary from 84 to 85%. On the other hand, the absolute transmittances of the MIM-A (black solid line) and the MIM-B (red solid line) devices, whose transmittances are seen to vary from 80 to 83%, are seen to be slightly decreased in comparison with the PET sample. The inset in Fig. 3 presents a photograph of an optically-transparent, mechanically-flexible, MIM-B memory device after bending.

Fig. 4 shows the current (semi-log scale)-voltage characteristics for (a) the MIM-A and (b) the MIM-B NVM devices. Fig. 4(a) shows that the hysteresis window of the I–V characteristics for the reference, MIM-A, device is negligible while Fig. 4(b) shows the presence of the large I–V hysteresis window for the MIM-B device, indicating that the charge storage capability of the devices can be attributed to the presence of the GQDs in the device. The voltage applied to both devices was swept from −2.5 to 5 V and vice versa. When the voltage for the MIM-B device was swept from 0 to −2.5 V, an abrupt increase in a current was observed at −1.7 V (V_{ON}), which switched the device from the low-current to the high-current state. The device remained in the high-current state when the voltage was swept from −2.5 to 0 V. When the bias polarity was changed from 0 to 5 V, the device switched from the high-current state to the low current state at 4.5 V. The device remained in the low-current state when the voltage was swept from 5 to 0 V.

Various conduction mechanisms, the Simmons and Verderber (SV) model [20], thermionic emission (TE) [15,21], Schottky emission [22], Poole-Frenkel (PF) emission [22] and the space-charge-limited-current (SCLC) mechanism [23–25], are typically proposed to explain the carrier transport behaviors in dielectric films. The SV model is unlikely to fit the obtained I-V curves due to the absence of an N-shaped I–V characteristic. TE is attributed to the heat-induced emission of electrons across a barrier. The Schottky and the PF emissions are general mechanisms used to explain the injection of charge carriers at metal-insulator interfaces [22,26]. In